GASTROENTEROLOGY 2007;132:1434–1446

BASIC–LIVER, PANCREAS, AND BILIARY TRACT

The Forkhead Transcription Factor FoxO1 Regulates Proliferation and Transdifferentiation of Hepatic Stellate Cells

MASAYUKI ADACHI,* YOSUKE OSAWA,* HIROSHI UCHINAMI,* TADAHIRO KITAMURA,‡ DOMENICO ACCILI,‡ and DAVID A. BRENNER*

*Department of Medicine and ‡Naomi Berrie Diabetic Center, Department of Medicine, College of Physicians and Surgeons of Columbia University, New York, New York

Background & Aims: **The Forkhead box gene, group O (FoxO) family of Forkhead transcription factors is phopsphorylated and inactivated by the phosphatidylinositol 3-kinase (PI3K)/AKT pathway and regulates a variety of cellular functions. Hepatic stellate cells (HSCs) play a crucial role in liver fibrosis. A fibrotic stimulus causes HSCs to transdifferentiate from a quiescent phenotype to a collagen-producing myofibroblast-like phenotype and to proliferate.** ***Methods:*** **Mutation/deletion mutants of FoxO1 were introduced into primary rat, mouse, and immortalized human HSCs and assessed for activation, proliferation, and signal transduction. The role of FoxO1 in experimental liver fibrosis was assessed in FoxO1$^{+/-}$ and FoxO1$^{+/+}$ mice.** ***Results:*** **Platelet-derived growth factor (PDGF) or insulin phosphorylates FoxO1 and induces FoxO1 translocation from the nuclei to the cytosol via the PI3K/AKT pathway in HSCs. Constitutively active FoxO1 inhibits proliferation via cell cycle arrest at the G1 phase, whereas dominant-negative FoxO1 enhances proliferation of HSCs even in the presence of the PI3K inhibitor LY294002. In addition, the phosphorylation of FoxO1 is increased during transdifferentiation of HSCs. The transdifferentiation is also inhibited by constitutively active FoxO1 and is accelerated by dominant-negative FoxO1. FoxO1 directly induces the expression of p27^{kip1} and manganese superoxide dismutase (MnSOD). After bile duct ligation for 3 weeks, FoxO1$^{+/-}$ mice are more susceptible to liver fibrosis, consistent with our in vitro results.** ***Conclusions:*** **FoxO1 plays a crucial role in the transdifferentiation and proliferation of HSCs in liver fibrosis. Hyperinsulinemia inactivates FoxO1 in HSCs, resulting in HSC activation and may result in the fibrosis in nonalcoholic fatty liver disease.**

Hepatic fibrosis is a wound-healing response to chronic liver injury, and hepatic stellate cells (HSCs) play a crucial role in this fibrotic response.[1] HSCs from normal liver show a quiescent phenotype storing vitamin A-rich fat droplets. During liver fibrosis, HSCs undergo an activation or a transdifferentiation process, which is characterized by loss of intracellular vitamin A stores and change to a myofibroblast-like cell with expression of α-smooth muscle actin (α-SMA). Transdifferentiated HSCs then remodel the extracellular matrix by secreting matrix metalloproteinases and depositing extracellular matrix, including type I collagen. In addition, HSCs migrate and proliferate in response to a variety of cytokines and growth factors elicited during liver injury. Therefore, transdifferentiation, proliferation, and collagen production of HSCs are key steps in liver fibrogenesis.

The phosphatidylinositol 3-kinase (PI3K)/AKT pathway is activated by growth factors and controls a variety of cellular responses, including survival, proliferation, and metabolism.[2] In HSC, the PI3K/AKT pathway is strongly activated by platelet-derived growth factor (PDGF), which is the most potent mitogen of HSC.[3–5] However, the precise mechanism by which the PI3K/AKT-signaling pathway regulates transdifferentiation and proliferation in HSCs is still unclear.

The Forkhead box gene, group O (FoxO) subfamily of Forkhead transcription factors comprises functionally re-

Abbreviations used in this paper: HSC, hepatic stellate cell; FoxO, Forkhead box gene, group O; MnSOD, manganese superoxide dismutase; PI3K, phosphatidylinositol 3-kinase; α-SMA, α-smooth muscle actin; ECM, extracellular matrix; PDGF, platelet-derived growth factor; PPAR-γ, peroxisome proliferator-activated receptor-γ; TIMP-1, tissue inhibitor of metalloproteinase-1; ROS, reactive oxygen species; NAFLD, nonalcoholic fatty liver disease; DAPI, 4′,6-diamidino-2-phenylindole, dihydrochloride.

0016-5085/07/$32.00
doi:10.1053/j.gastro.2007.01.033

lated proteins FoxO1, FoxO3a, and FoxO4 and plays an important role in metabolism, differentiation, survival, and proliferation.[6] AKT-catalyzed phosphorylation of FoxO1 results in nuclear exclusion and inhibition of FoxO-dependent gene expression.[7] Because FoxO factors regulate proliferation and tumor growth in a variety of cells,[8,9] it is possible that FoxO1 participates in HSC proliferation downstream of the PI3K/AKT pathway.

HSC transdifferentiation induces profound morphologic and molecular changes. Transdifferentiated HSCs express α-SMA and the myogenic transcription factor MyoD,[10] whereas quiescent HSCs express adipocytic peroxisome proliferator-activated receptor-γ (PPAR-γ).[11,12] These findings raise the possibility that HSCs undergo transdifferentiation from an adipocytic phenotype into a myofibroblastic phenotype. Because FoxO factors control cellular differentiation including adipocytes and myoblasts,[13–15] it is possible that FoxO1 participates in the transdifferentiation process of HSCs.

The present study evaluates the role of FoxO1 in proliferation and transdifferentiation of HSCs. Our functional analysis of FoxO1 revealed that both proliferation and transdifferentiation of HSCs were inhibited by transcriptionally active FoxO1 and enhanced by transcriptionally inactive FoxO1. Moreover, mice of FoxO1 haploinsufficiency ($FoxO1^{+/-}$) were more sensitive to experimental liver fibrosis. Our study identifies FoxO as a key transcription factor that regulates hepatic fibrogenesis.

Materials and Methods

Cell Cultures and Treatments

Primary HSCs were isolated from male Sprague-Dawley rats and male Balb/c mice. Primary HSCs were isolated by a 2-step perfusion using pronase E (EMD Chemicals, Gibbstown, NJ) and collagenase D (Roche, Mannheim, Germany), followed by Nycodenz (Axis-Shield, Oslo, Norway) 2-layer discontinuous density gradient centrifugation as previously described.[16] Purity of rat or mouse HSC preparations was 96% and 97%, respectively, as assessed by autofluorescence at day 1. HSCs were cultured on uncoated plastic tissue culture dishes in Dulbecco's modified Eagle medium (DMEM) supplemented with 10% fetal bovine serum (FBS). Growth medium was changed daily. Rat HSCs were passaged once between days 5 and 7 when cells were culture activated. The fully transdifferentiated rat HSCs were used for experiments between days 10 and 14. Mouse HSCs were not passaged and were used for experiments on days 0 to 4. In some experiments, immortalized human HSC line hTERT HSCs were cultured in DMEM supplemented with 10% FBS as previously described.[17] Primary rat HSCs or hTERT HSCs were serum starved in serum-free DMEM for 24 hours and were treated with 20 ng/mL PDGF-BB (Roche) or 100 nmol/L insulin (Invitrogen, Auckland, New Zealand). Where indicated in results, cells were preincubated with 20 μmol/L LY294002 (Sigma-Aldrich, St. Louis, MO) for 1 hour.

Adenoviruses

The adenoviral vectors encoding hemagglutinin (HA)-tagged wild-type FoxO1 (WT-FoxO1), HA-tagged constitutively active FoxO1 (ADA-FoxO1), HA-tagged dominant-negative FoxO1 (Δ256-FoxO1), HA-tagged constitutively active AKT (Myr-AKT), HA-tagged dominant-negative AKT (DN-AKT), manganese superoxide dismutase (MnSOD), green fluorescent protein (GFP), and bacterial β-galactosidase (LacZ) have been previously described.[14,16,18–20] ADA-FoxO1 contains mutation in all of the 3 AKT phosphorylation sites, resulting in constitutively active FoxO1-dependent gene transcription.[19] Δ256-FoxO1 contains a DNA-binding domain but lacks a transactivation domain, resulting in inhibition of FoxO1-dependent gene transcription.[19] The adenovirus vector encoding $p27^{kip1}$ short interfering RNA (siRNA) was created by using the pRNAT-H1.1/Adeno shuttle vector (GenScript, Piscataway, NJ) and AdEasy Adenoviral Vector System (Stratagene, La Jolla, CA) according to the manufacturers' protocol. Oligonucleotide sequences were modified from the sequences by Tamamori-Adachi M et al[21]: 5′-CGC GTG TGG GAG TGT TTA ATG GGA ACG TGT GCT GTC CGT TCC CGT TAG ACA CTC TCA CTT TTT A-3′ and 5′-AGC TTA AAA AGT GAG AGT GTC TAA CGG GAA CGG ACA GCA CAC GTT CCC ATT AAA CAC TCC CAC A-3′. Cells were transduced with each adenovirus at a multiplicity of infection (MOI) of 100 (primary mouse HSCs), 200 (primary rat HSCs or hTERT HSCs), or otherwise instructed to achieve transduction rates of greater than 80%.

^{3}H-Thymidine Incorporation Assay

DNA synthesis was estimated as the amount of methyl-^{3}H-thymidine as previously described.[22] HSCs were incubated with 1 μCi/mL ^{3}H-thymidine (Amersham, Piscataway, NJ) for 18 or 24 hours followed by trichloroacetic precipitation, lysis, and measurement in a scintillation counter.

Fluorescent-Activated Cell Sorting Analysis

Twenty-four hours after treatment with PDGF or insulin, rat HSCs were harvested by scraping and fixed with cold ethanol (50%) in phosphate-buffered saline (PBS) for 1 hour. Cells were then washed with PBS and treated with 0.5 mg/mL RNase A (Qiagen, Valencia, CA) for 1 hour at 37°C. Cells were incubated with 20 μg/mL propidium iodide (Sigma-Aldrich) at 4°C in the dark, and cell cycle state was assessed by flow cytometry using a fluorescent-activated cell sorting (FACS) instrument (FACSCalibur, BD Biosciences, San Jose, CA).

Western Blot Analysis and Immunoprecipitation

Electrophoresis of protein extracts and subsequent blotting were performed as previously described.[18] Blots were incubated with antibodies against phospho-FoxO1 (Ser-256), phospho-AKT (Ser-473), hemagglutinin (both Cell Signaling, Beverly, MA), FoxO1, AKT (both Santa Cruz, Santa Cruz, CA), $p27^{kip1}$ (BD Biosciences), MnSOD (Stressgen, Victoria BC, Canada), α-SMA, β-actin (both Sigma-Aldrich), and desmin (DAKO, Glostrup, Denmark) overnight at 4°C. For detection of insulin receptor substrate-2 (IRS-2) tyrosine phosphorylation, cell lysates from insulin-treated rat HSCs were immunoprecipitated with anti-IRS-2 antibody (Upstate, Lake Placid, NY) and protein A-agarose (Santa Cruz). Immunoprecipitates were then subjected to SDS-PAGE, and Western blot analysis was performed using antiphosphotyrosine antibody (Upstate) or anti-IRS-2 antibody.

Immunofluorescence Cell Staining

One hour after the treatment with PDGF or insulin, primary rat HSCs were fixed with −10°C methanol for 5 minutes and blocked with PBS containing 4% FBS. Cells were incubated with anti-HA antibody for 1 hour and then incubated with rhodamine-conjugated anti-mouse IgG antibody (Pierce, Rockford, IL). For nuclear counterstaining, 4',6-diamidino-2-phenylindole, dihydrochloride (DAPI; Molecular Probes, Eugene, OR) was used according to the manufacturer's instruction. Cells were observed under a fluorescence microscope with appropriate filters.

Determination of Intracellular Reactive Oxygen Species Production in HSCs

Reactive oxygen species (ROS) production was tested in activated HSCs using 5-(and-6)-chloromethyl-2′,7′-dichlorodihydrofluorescein diacetate, acetyl ester (CM-H_2DCFDA)-based fluorescence. DCFDA-associated ROS production was measured in a time course of 30 minutes using multiwell platereader (BMG Optima, Durham, NC).[23]

Quantitative Real-Time Reverse-Transcriptase Polymerase Chain Reaction

Extracted RNA from the liver and the cells was reverse transcribed (First-Strand cDNA Synthesis Kit; Amersham), and quantitative real-time polymerase chain reaction (PCR) with the probe-primers sets of human $p27^{kip1}$ (Hs00153277_m1), mouse $p27^{kip1}$ (Mm00438167_g1), human MnSOD (SOD2, Hs00167309_m1), mouse MnSOD (Mm00449726_m1), mouse collagen α1(I) (Mm00801666_g1), mouse PPAR-γ (Mm00440945_m1), mouse TIMP-1 (Mm00801666_g1), and 18S ribosomal RNA (Hs99999901_s1) (Applied Biosystems, Foster City, CA) was performed using Taqman analysis (ABI Prism 7000 Sequence Detection System, Applied Biosystems). The changes were normalized to 18S.

Chromatin Immunoprecipitation Assay

Chromatin immunoprecipitation (ChIP) assays were performed by using the ChIP assay kit (Upstate) with some modification as previously described.[24] hTERT HSCs were transduced with WT-FoxO1 or ADA-FoxO1 adenoviruses. ChIP was performed with anti-HA antibody or normal mouse IgG as a negative control. Precipitated DNA was analyzed by PCR using specific primers for promoter regions containing the Forkhead binding element (FBE) of $p27^{kip1}$: 5′-TGCGCGCTCCTAGAGCTC-3′ and 5′-TTTCTCCCGGGTCTGCAC-3′, MnSOD: 5′-GTCCCAGCCTGAATTTCC-3′ and 5′-CTAGGCTTCCGGTAAGTG-3′, and β-actin coding region: 5′-CAAGAGATGGCCACGGCTGC-3′ and 5′-CTAGAAGCATTTGCGGTGGACG-3′.[25]

Animal Studies

$FoxO1^{+/-}$ mice and wild-type littermates ($FoxO1^{+/+}$ mice) (mixed background) were bred for studies as previously described.[26] Liver fibrosis was induced by bile duct ligation (BDL).[23] The mice were killed 3 weeks after BDL, and collagen α1(I) mRNA levels and protein levels for α-SMA and desmin were determined as previously described.[23] Collagen deposition was stained with Sirius red (saturated picric acid containing 0.1% Direct Red 80 and 0.1% FastGreen FCF). For measurement of hydroxyproline content, the extracted protein from the liver was hydrolyzed for 24 hours at 110°C in 6 mol/L HCl. The samples were oxidized with Chloramine-T (Sigma-Aldrich) for 25 minutes and then incubated with Ehrich's percholic acid solution containing 4-(Dimethylamino)benzaldehyde (Sigma-Aldrich) at 65°C for 20 minutes. The sample absorbance was measured at 560 nm. The acute liver injury produced by anti-Fas antibody (Jo2; BD Pharmingen, San Diego, CA) was also assessed in $FoxO1^{+/-}$ and $FoxO1^{+/+}$ mice. Jo2 (100 μg/mouse) was administrated intravenously. Treated animals were anesthetized and killed 2.5 hours after Jo2 administration. All procedures for HSC isolation and BDL were approved by the Investigation and Ethics Committee and Institutional Animal Care and Use Committee of the Columbia University.

Statistical Analysis

Results are expressed as mean ± SD. The results were analyzed using the unpaired Student t test. A P value of less than .05 was considered statistically significant.

Results

PDGF or Insulin Phosphorylates FoxO1 in Transdifferentiated Primary Rat HSCs

Because the PI3K/AKT pathway induces proliferation and migration of HSCs,[4,5] we first sought to eluci-

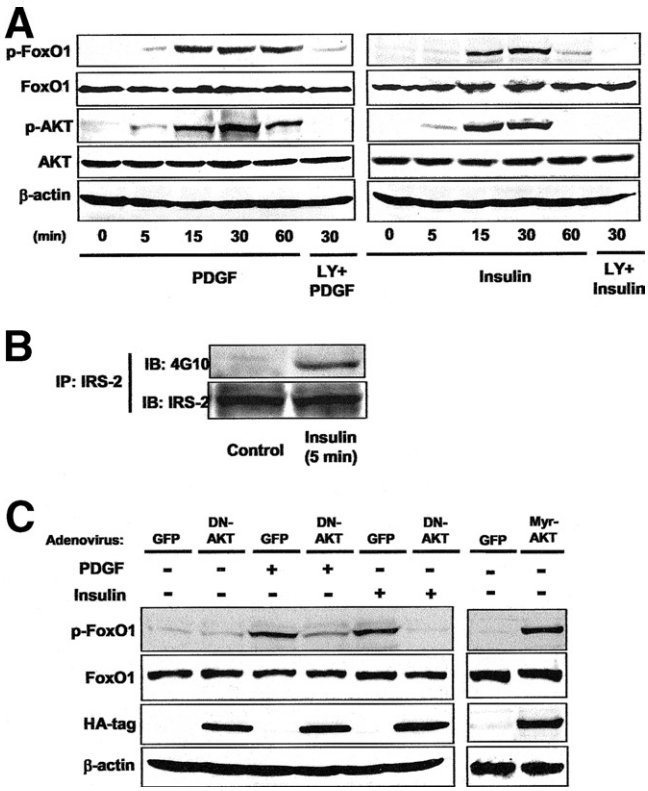

Figure 1. Activation of PI3K/AKT pathway phosphorylates FoxO1. (*A*) Primary rat HSCs were pretreated with (LY+) or without 20 μmol/L of LY294002 for 1 hour. HSCs were then treated with 20 ng/mL PDGF or 100 nmol/L insulin for the indicated time periods. FoxO1, phospho-FoxO1, AKT, phospho-AKT, and β-actin were analyzed by Western blot analysis. (*B*) IRS-2 was immunoprecipitated (IP) using anti-IRS-2 antibody, and tyrosine phosphorylation was determined by Western blot analysis (IB) using antiphosphortyrosine (pY) antibody. IRS-2 mass was determined by reprobing the blot with anti-IRS-2 antibody. (*C*) Rat HSCs were transduced with indicated adenoviruses for 24 hours. Serum-starved HSCs were then treated with (+) or without (−) PDGF or insulin for 30 minutes. FoxO1, phospho-FoxO1, HA, and β-actin were analyzed by Western blot analysis. The results shown are representative of 3 independent experiments.

date the role of FoxO1 in the proliferation of transdifferentiated HSCs. PDGF (20 ng/mL) or insulin (100 nmol/L) induced phosphorylation of FoxO1 in parallel with AKT phosphorylation in serum-starved primary rat HSCs. The phosphorylation of FoxO1 or AKT was completely inhibited by the pretreatment with PI3K inhibitor LY294002 (Figure 1*A*). Insulin also phosphorylated IRS-2 (Figure 1*B*). Moreover, phosphorylation of FoxO1 by PDGF or insulin was completely inhibited by overexpression of a dominant-negative form of AKT (DN-AKT) (Figure 1*C*, *left*). In contrast, constitutively active AKT-transduced HSCs induce phosphorylation of FoxO1 during serum starvation (Figure 1*C*, *right*). These results indicate that PDGF or insulin induces phosphorylation of endogenous FoxO1 via the PI3K/AKT pathway in primary rat HSCs.

PDGF or Insulin Induces Nuclear Exclusion of FoxO1 in Transdifferentiated Primary Rat HSCs

AKT-dependent phosphorylation of FoxO transcription factors induces nuclear exclusion, resulting in inhibition of their transcriptional activity.[27,28] To investigate the subcellular distribution of FoxO1 after PDGF or insulin, we transduced rat HSC with WT-FoxO1 or ADA-FoxO1 and immunostained with anti-HA antibody. In serum-starved HSCs, FoxO1 protein had a nuclear distribution (Figure 2*A*). Addition of PDGF or insulin resulted in a cytosolic redistribution of FoxO1, which was blocked by LY294002 (Figure 2*A*). Phosphorylation-resistant ADA-FoxO1 showed nuclear localization even after PDGF or insulin (Figure 2*B* and *C*). These results indicate that PDGF- or insulin-induced FoxO1 phosphorylation results in nuclear exclusion of FoxO1 via the PI3K/AKT pathway.

FoxO1 Inhibits Proliferation by G1 Arrest of Cell Cycle in Transdifferentiated Primary Rat HSCs

To investigate the role of FoxO1 in the proliferation of HSCs, ^{3}H-thymidine incorporation was assessed. PDGF or insulin increased ^{3}H-thymidine incorporation, which was significantly inhibited in ADA-FoxO1-transduced HSCs (Figure 3*A*). In contrast, HSCs transduced with Δ256-FoxO1 showed an increase in ^{3}H-thymidine incorporation (Figure 3*B*), and PDGF or insulin did not further increase ^{3}H-thymidine in Δ256-FoxO1-transduced cells (data not shown). LY294002 inhibited PDGF- or insulin-induced ^{3}H-thymidine incorporation, whereas Δ256-FoxO1 reversed this inhibition (Figure 3*B*), indicating that FoxO1 is a crucial downstream target of the PI3K/AKT pathway to control HSC proliferation. To investigate further the mechanisms by which FoxO1 controls proliferation, FACS analyses were performed to examine the cell cycle. PDGF, insulin or Δ256-FoxO1 induced cells to accumulate in the S/G2/M phase of the cell cycle. In contrast, ADA-FoxO1 resulted in the accumulation of cells in the G0/G1 phase, even after treatment with PDGF or insulin (Figure 3*C* and *D*). These results indicate that active (nuclear) FoxO1 inhibits proliferation by inducing cell cycle arrest in the G1 phase.

$p27^{kip1}$ and MnSOD Are Transcriptional Targets of FoxO1 That Regulate Proliferation in HSCs

FoxO factors control a variety of target genes, including antioxidant genes[29] and regulators of metabolism,[19] cell cycle,[9,30] and cell death.[7,31] To investigate the mechanism by which FoxO1 inhibits proliferation via cell cycle arrest at G1, target genes of FoxO1 were assessed with hTERT HSCs.[17] hTERT HSCs showed the same results as shown in primary rat HSCs, includ-

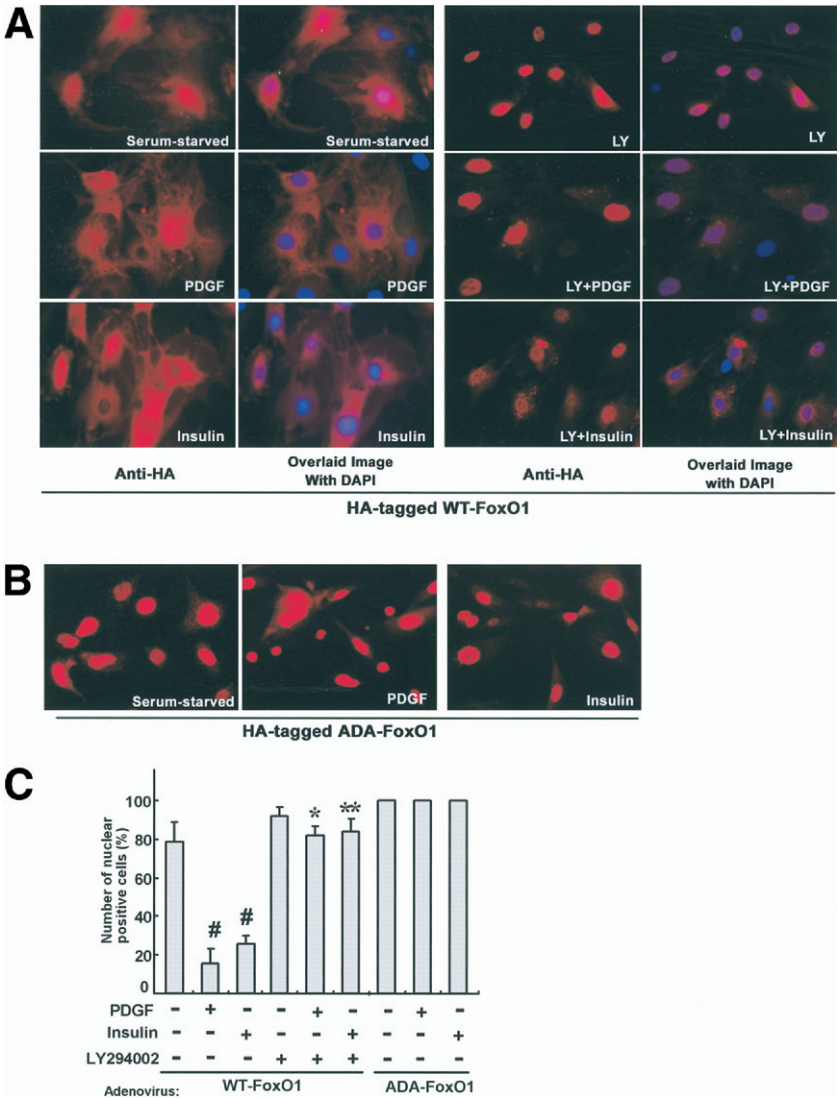

Figure 2. PDGF or insulin induces subcellular translocation of FoxO1. (*A*) Rat HSCs were transduced with WT-FoxO1 and were treated with PDGF or insulin for 30 minutes in the absence or presence (LY+) of LY294002. After fixation, immunofluorescence staining for HA was performed with DAPI staining. *Left panels* indicate WT-FoxO1 (rhodamine), and *right panels* indicate merged images of WT-FoxO1 and DAPI. (*B*) Immunofluorescence staining for ADA-FoxO1. The results shown are representative of at least 3 independent experiments. (*C*) Quantitation of cells exhibiting positive nuclear staining (combination of cell exhibiting either nuclear staining only or cells exhibiting both nuclear and cytoplasmic staining) was determined by counting a total of 10 randomly prechosen fields. $^{\#}P < .01$ vs nonstimulated WT-FoxO1-transduced cells, $^{*}P < .01$ vs PDGF-stimulated WT-FoxO1-transduced cells, $^{**}P < .05$ vs insulin-stimulated WT-FoxO1-transduced cells by using the Student t test.

ing phosphorylation of FoxO1 by PDGF or insulin and inhibition of proliferation by ADA-FoxO1 (data not shown). Among the FoxO1 target genes tested, $p27^{kip1}$ and MnSOD were significantly decreased by PDGF, insulin, or Δ256-FoxO1. In contrast, ADA-FoxO1 markedly increased mRNA levels of $p27^{kip1}$ and MnSOD, which were not inhibited by PDGF or insulin (Figure 4*A* and see Supplemental Figure 1 online at www.gastrojournal.org). These changes in $p27^{kip1}$ and MnSOD expression were confirmed at the protein level (Figure 4*B*). ChIP assays demonstrated that WT-FoxO1 binds to the promoter regions of $p27^{kip1}$ and MnSOD genes in serum-starved hTERT HSCs. This binding to the promoter regions was inhibited by PDGF or insulin (Figure 4*C*). In contrast, DNA binding of phosphorylation-resistant ADA-FoxO1 was not inhibited by PDGF or insulin. To address whether $p27^{kip1}$ and MnSOD regulate HSC proliferation as a downstream target of FoxO1, we used adenoviruses that transduce $p27^{kip1}$ short hairpin (shRNA) or MnSOD. $p27^{kip1}$ shRNA effectively abolished the inhibitory effect of ADA-FoxO1 on HSC proliferation, suggesting that $p27^{kip1}$ is a downstream target of FoxO1 (Figure 5*B*). PDGF produced intracellular ROS in rat HSCs, as measured by DCFDA fluorescence. Transduction of MnSOD inhibited both PDGF-induced ROS produc-

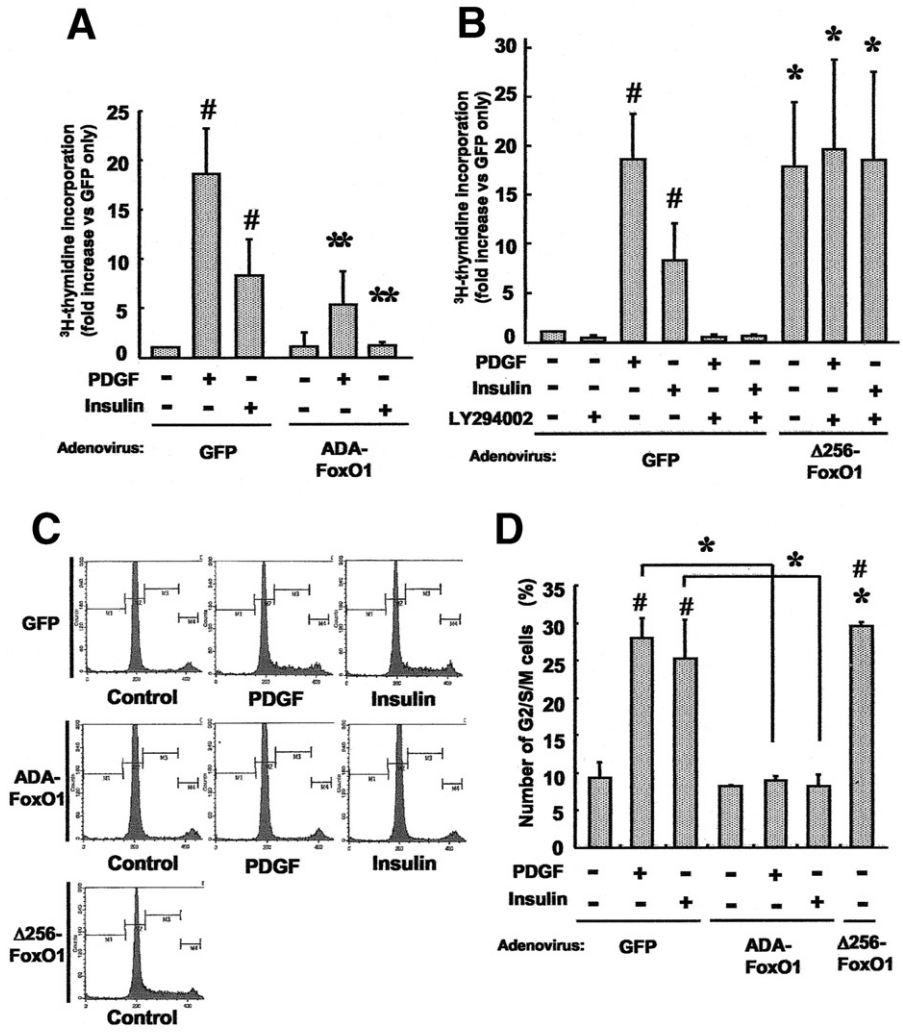

Figure 3. FoxO1 inhibits PDGF- or insulin-induced proliferation by G0/G1 cell arrest in rat HSCs. HSCs were transduced with ADA-FoxO1 in (*A*) and Δ256-FoxO1 in (*B*) or GFP as control. Twenty-four hours after the transduction, HSCs were incubated under serum-free media for 24 hours. After the preincubation with (+) or without (−) LY294002 for 1 hour, cells were stimulated with (+) or without (−) PDGF or insulin for 6 hours. Cells were then incubated with 1 μCi/mL methyl-^{3}H-thymidine for an additional 18 hours, and DNA synthesis was assessed. Data were expressed as the mean ± SD from 3 independent experiments. (*C*) Rat HSCs were transduced with indicated adenoviruses for 24 hours. Rat HSCs were then serum starved for additional 24 hours and stimulated without (*control*) or with PDGF or insulin. Twenty-four hours after the stimulus, FACS analysis was performed. Representative FACS scan charts from 3 independent experiments are shown. (*D*) A graphical representation of the FACS data is shown. Data are expressed as the mean ± SD from 3 independent experiments. #$P < .01$ vs nonstimulated GFP-transduced cells; *$P < .01$, **$P < .05$ vs GFP-transduced cells by using the Student *t* test.

tion (Figure 5*C*) and PDGF-induced proliferation, suggesting critical roles of ROS and MnSOD in PDGF-induced HSC proliferation (Figure 5*D*). In contrast, insulin did not significantly increase intracellular ROS in rat HSCs, and transduction of MnSOD did not inhibit insulin-induced HSC proliferation (Figure 5*C* and *D*). These results suggest that the role of MnSOD in HSC proliferation is affected only by PDGF.

Collectively, these results suggest that $p27^{kip1}$ and MnSOD are specific transcriptional targets of FoxO1 in HSCs. PDGF or insulin attenuated the binding of FoxO1 onto the $p27^{kip1}$ and MnSOD promoter regions, resulting in inhibition of their transcription.

FoxO1 Inhibits Transdifferentiation of Freshly Isolated Mouse HSCs

Because FoxOs control cellular differentiation including that of adipocytes and myoblasts,[14,15] we next tried to elucidate whether FoxO1 regulates the transdifferentiation process of HSCs. Mouse HSCs were isolated and culture activated in 10% FBS-containing media. The α-SMA expression and the phosphorylation status of FoxO1 were increased in day 4 as compared with day 0 and day 2 HSCs (Figure 6*A*). Moreover, messenger RNA (mRNA) levels of $p27^{kip1}$ and MnSOD were decreased in day 4 HSCs compared with day 2 HSCs (Figure 6*B*). Δ256-FoxO1-transduced HSCs showed an accelerated

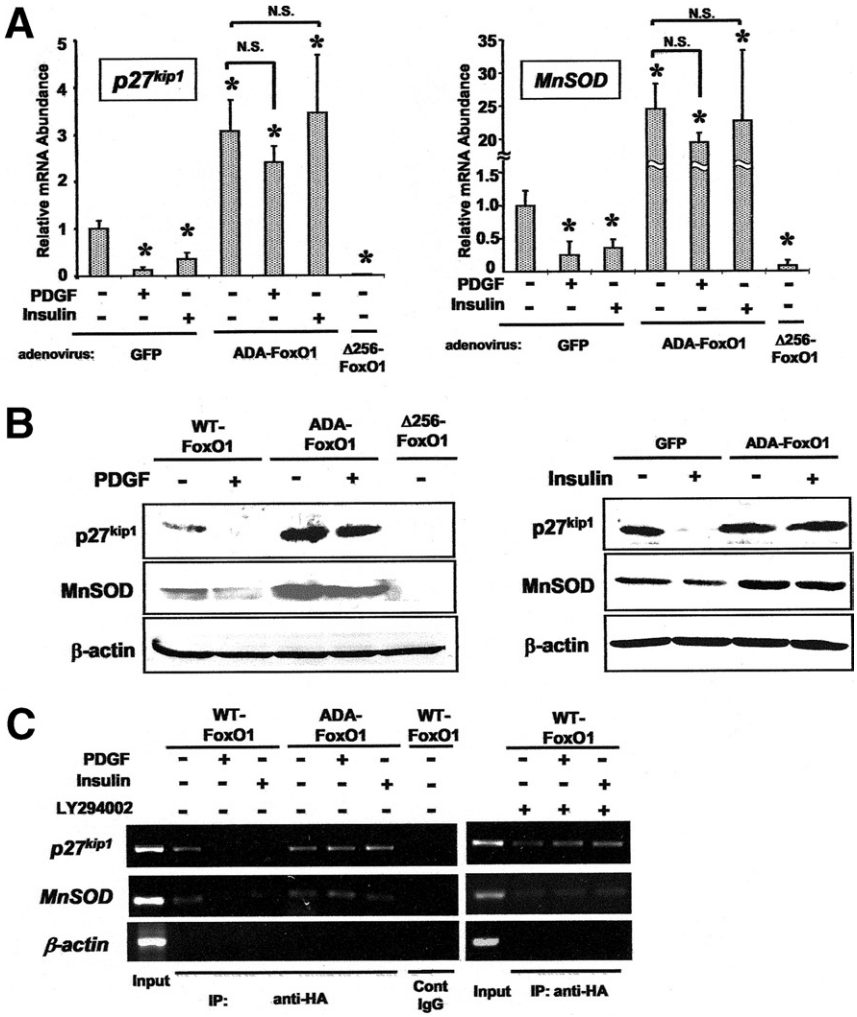

Figure 4. p27^{kip1} And MnSOD are transcriptional targets of FoxO1 in HSCs. hTERT HSCs were transduced with indicated adenoviruses for 24 hours. Cells were then serum starved for additional 24 hours. (*A*) Cells were treated with (+) or without (−) PDGF or insulin for 2 hours, and mRNA levels of p27^{kip1} and MnSOD were determined by quantitative real-time RT-PCR. Data are expressed as the mean ± SD from 3 independent experiments. *$P < .01$ vs nonstimulated GFP-hTERT HSCs. (*B*) hTERT HSCs were treated with (+) or without (−) PDGF or insulin for 18 hours, and protein extracts were then subjected to Western blot analysis for p27^{kip1} and MnSOD. The results shown are representative of at least 3 independent experiments. (*C*) After preincubation with (+) or without (−) LY294002 for 1 hour, hTERT HSCs were treated with (+) or without (−) PDGF or insulin for 1 hour, and ChIP assay was performed. Cross-linked DNA-protein complex was immunoprecipitated (IP) with anti-HA antibody or normal mouse IgG (Cont IgG). Immunoprecipitated DNA was analyzed by PCR using specific primer sets for promoter regions of p27^{kip1} and MnSOD or β-actin coding region. The results shown are representative of 3 independent experiments. NS, not significant.

change into myofibroblast-like appearance as compared with GFP-transduced HSCs in day 4 (Figure 6*C*; a, c, d, and f). In contrast, a vitamin A-containing quiescent phenotype was maintained in ADA-FoxO1-transduced HSCs in day 4 (Figure 6*C*; b and e). Moreover, the expression of α-SMA was inhibited by ADA-FoxO1 and enhanced by Δ256-FoxO1 (Figure 6*D*). These results indicate that ADA-FoxO1 inhibits and Δ256-FoxO1 accelerates HSC transdifferentiation.

PPAR-γ is expressed in the quiescent HSCs, and its expression decreases after HSC transdifferentiation.[11,12,32] Tissue inhibitor of metalloproteinase-1 (TIMP-1) is not expressed in the quiescent HSCs, and its expression increases after HSC transdifferentiation.[33] As we predicted, ADA-FoxO1-transduced HSCs showed higher PPAR-γ and lower TIMP-1 mRNA levels as compared with GFP-transduced HSCs, whereas Δ256-FoxO1-transduced HSCs showed lower PPAR-γ levels (Figure 6*E*). Moreover, mRNA levels of collagen α1(I) were increased in Δ256-FoxO1-transduced HSCs and decreased in ADA-FoxO1-transduced HSCs (Figure 6*E*). These changes in PPAR-γ, TIMP-1, and collagen α1(I) expressions by ADA-FoxO1 were likely to be due to an overall inhibitory effect of FoxO1 on HSC transdifferentiation rather than FoxO1-mediated transcriptional up-regulation because the Forkhead binding element was not found in the promoter regions of these genes (data not shown).

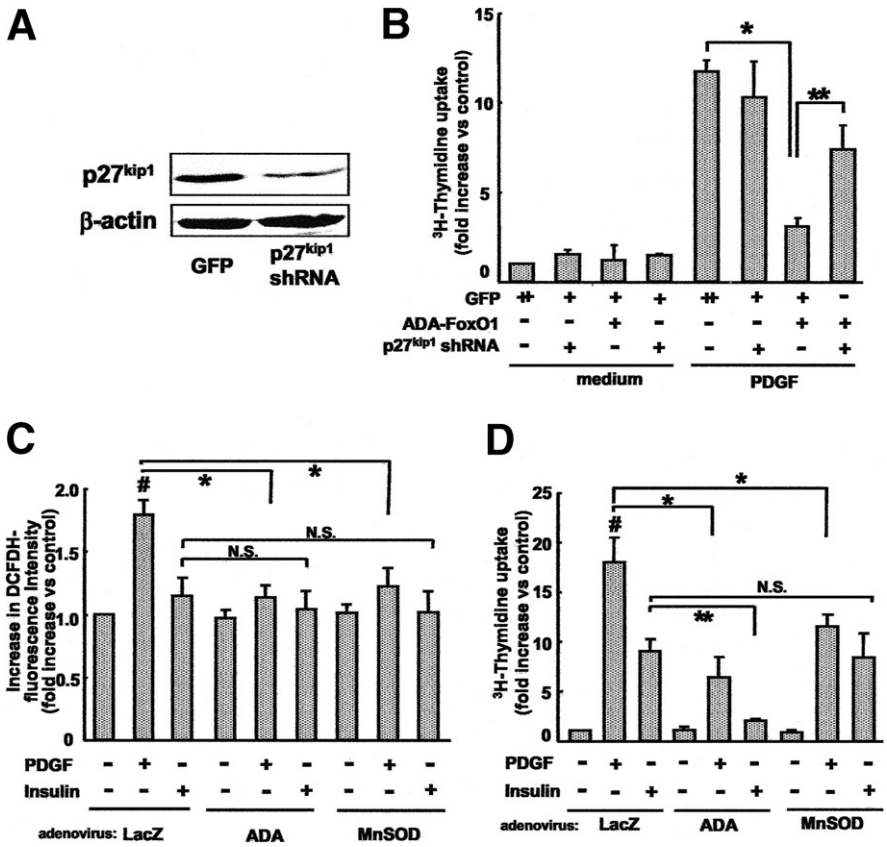

Figure 5. p27^{kip1} And MnSOD play a critical role in HSC proliferation. (*A* and *B*) Rat HSCs were transduced with indicated adenoviruses at MOI of 150 (+) or 300 (++). Twenty-four hours after transduction, HSCs were incubated under serum-free media for 24 hours. (*A*) Protein extracts were then subjected to Western blot analysis for p27^{kip1}. The results shown are representative of at least 3 independent experiments. (*B*) Cells were then stimulated with (+) or without (−) PDGF or insulin for 24 hours, and DNA synthesis was assessed. *$P < .01$ vs GFP (300 MOI)-transduced cells, **$P < .05$ vs GFP+ADA-FoxO1 (150 + 150 MOI)-transduced cells by using the Student *t* test. (*C* and *D*) Rat HSCs were transduced with MnSOD, ADA-FoxO1, or LacZ. Twenty-four hours after transduction, HSCs were incubated under serum-free media for 24 hours. (*C*) DCFDA-associated ROS production immediately after treatment with PDGF or insulin was measured in a time course of 30 minutes using a multiwell plate reader. Cells were stimulated with (+) or without (−) PDGF or insulin for 18 hours, and DNA synthesis was assessed. Data are expressed as the mean ± SD from 3 independent experiments. #$P < .05$ vs nonstimulated GFP-transduced cells, *$P < .05$ vs GFP + PDGF, **$P < .05$ vs GFP + insulin by using the Student *t* test. NS, statistically not significant.

FoxO1 Inhibits Proliferation of Mouse HSCs During Transdifferentiation

Although the proliferative ability of mouse transdifferentiated HSCs is less than that of rat transdifferentiated HSCs (data not shown), mice HSCs started to proliferate within day 4 (Figure 7*A*). The proliferation of transdifferentiating mouse HSCs was increased in Δ256-FoxO1-transduced HSCs, whereas it was inhibited in ADA-FoxO1-transduced HSCs (Figure 7*A* and *B*). FACS analysis demonstrated that Δ256-FoxO1-transduced HSCs increased in number of cells in the S/G2/M phase of the cell cycle, whereas ADA-FoxO1-transduced HSCs resulted in accumulation in the G0/G1 phase (Figure 7*C*). These results suggest that FoxO1 also controls proliferation of HSCs not only in the transdifferentiated state but also in the transdifferentiation process.

FoxO1$^{+/-}$ Mice Are Sensitive to Experimental Liver Fibrosis

Because FoxO1 inhibits HSC transdifferentiation and proliferation, we hypothesized that loss of FoxO1 would increase liver fibrosis in vivo. Because FoxO1$^{-/-}$ mice have embryonic lethality,[34] a model of secondary biliary fibrosis was performed in FoxO1$^{+/-}$ and wild-type FoxO1$^{+/+}$ mice. Sham-operated FoxO1$^{+/-}$ mice did not show any histologic differences from FoxO1$^{+/+}$ mice (data not shown). After 3 weeks of bile duct ligation, Sirius red staining demonstrated markedly increased liver fibrosis in FoxO1$^{+/-}$ mice as compared with FoxO1$^{+/+}$ mice (Figure 8*A* and *B*). Consistent with histologic analysis, FoxO1$^{+/-}$ mice showed increased hepatic levels of hydroxyproline and collagen α1(I) mRNA (Figure 8*C* and *D*). Moreover, α-SMA and desmin expressions were increased in bile duct-ligated FoxO1$^{+/-}$ mice (Figure 8*F*). In contrast, FoxO1$^{+/-}$ and FoxO1$^{+/+}$ mice showed similar

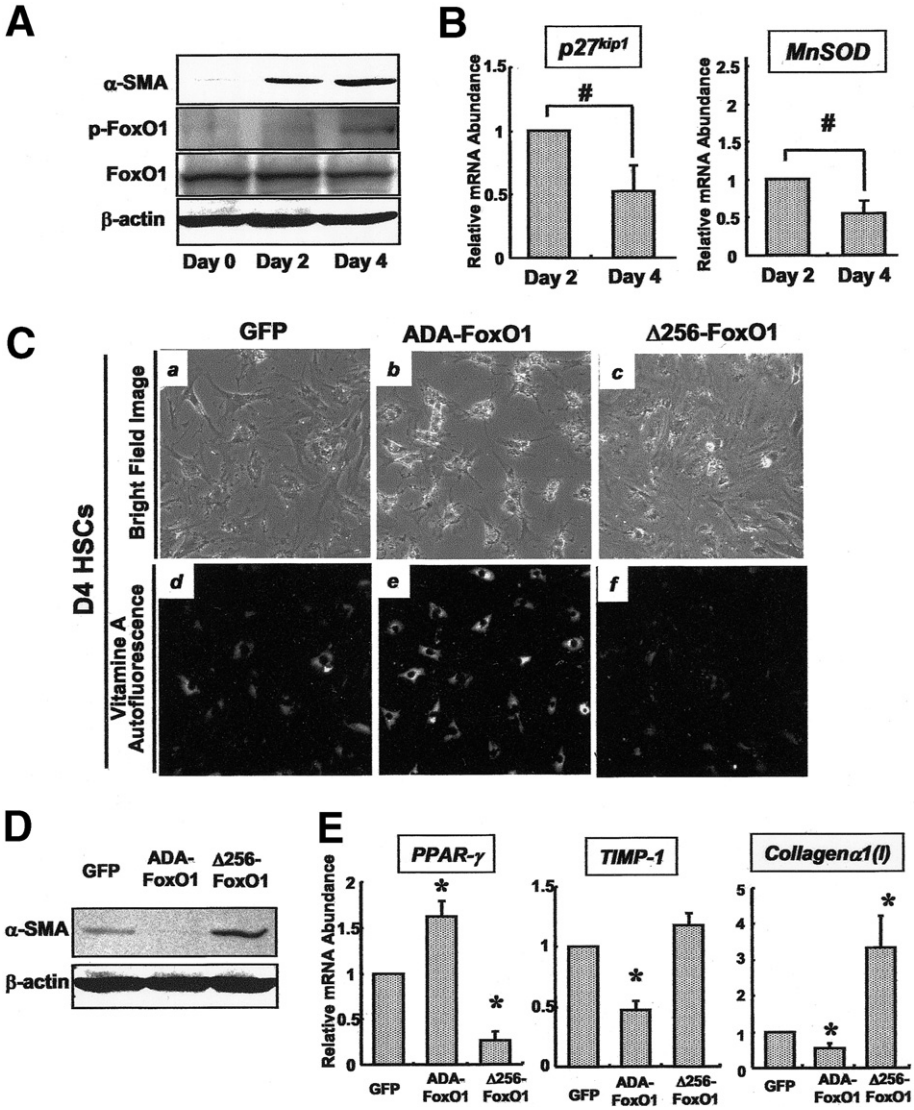

Figure 6. FoxO1 regulates HSC transdifferentiation. Mouse HSCs were isolated and culture activated under 10% FBS-containing media. Cells were transduced with indicated adenoviruses on day 1 (*C–E*). (*A*) Culture media were refreshed every day, and whole cell extracts were collected at indicated time points. Culture media were refreshed 2 hours prior to the protein extraction. α-SMA, phospho-FoxO1, FoxO1, and β-actin were analyzed by Western blot analysis. (*B*) mRNA levels of $p27^{kip1}$ and MnSOD on day 2 and day 4 HSCs were determined by quantitative real-time RT-PCR. Data are expressed as the mean ± SD from 3 independent experiments. #$P < .01$ vs day 2 HSCs by using the Student *t* test. (*C*) Characteristic morphorologic changes during HSC transdifferentiation were observed under fluorescent microscopy on day 4. Phase-contrasted micrographs (*a–c*) and vitamin A autofluorescences (*d–f*) were shown. Original magnifications, 200×. (*D*) Western blot analysis for α-SMA and β-actin on day 2 HSCs. The results shown are representative of 3 independent experiments. (*E*) mRNA levels of PPAR-γ, TIMP-1, and collagen α1(I) on day 4 HSCs were determined by quantitative real-time RT-PCR. Data are expressed as the mean ± SD from 3 independent experiments. *$P < .01$ vs GFP-transduced cells by using the Student *t* test.

liver injury at an earlier time point after bile duct ligation (Figures 8 and 9*E*) and after the acute liver injury of anti-Fas antibody (Jo-2) treatment (see Supplemental Figure 2*A* and *B* online at www.gastrojournal.org). Because there are no targeted HSC gene knockout mice, the cell type responsible for the increased hepatic fibrosis in the FoxO1 heterozygous mice cannot be identified. However, these results demonstrate that decreased FoxO1 increases experimental liver fibrosis, consistent with our cell culture studies.

Discussion

The present study demonstrates that (1) PDGF or insulin phosphorylates FoxO1 via the PI3K/AKT pathway in transdifferentiated HSCs, result in FoxO1 translocation from the nucleus to the cytosol; (2) FoxO1 is phosphorylated during the transdifferentiation of quiescent primary HSCs; (3) proliferation and transdifferentiation of HSCs are inhibited by transcriptionally active ADA-FoxO1 and enhanced by transcriptionally inactive Δ256-FoxO1; (4)

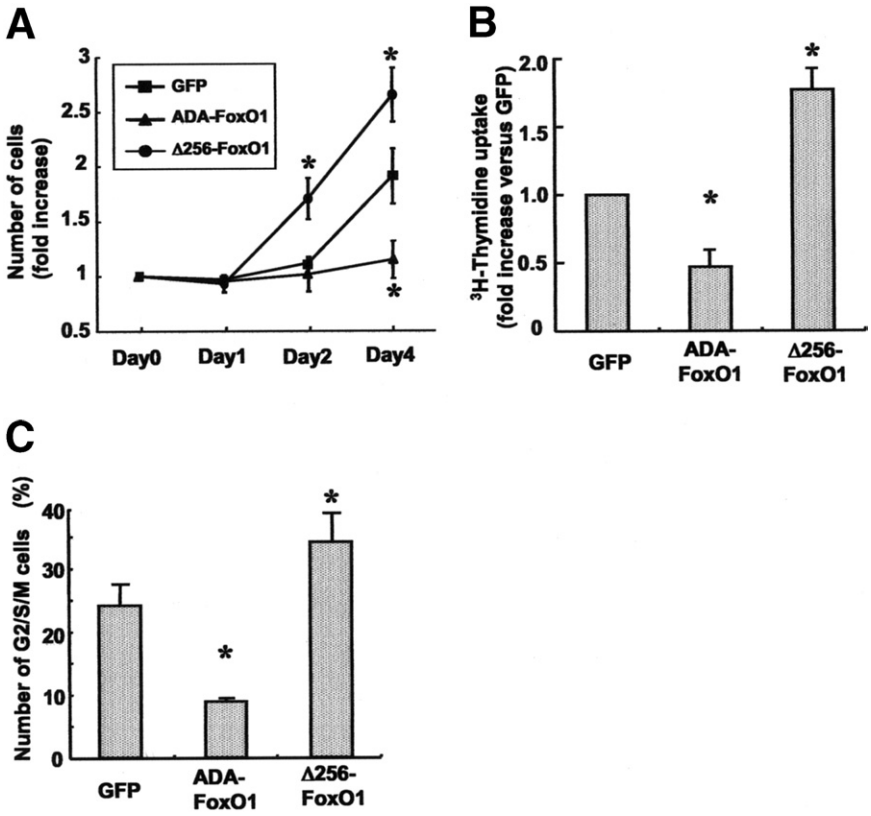

Figure 7. FoxO1 inhibits proliferation in transdifferentiating mouse HSCs. HSCs were transduced with indicated adenoviral vectors on day 1. (*A*) Number of HSCs was determined under the microscopic fields at indicated time points. Number of cells within a field of view at a magnification of 400× was determined. Averages were obtained from 5 randomly prechosen fields. (*B*) On day 3, 1 μCi/mL methyl-^{3}H-thymidine was added and incubated for 24 hours, and then DNA synthesis was assessed. (*C*) FACS analysis was performed using day 4 HSCs. The percentage of G2/S/M cells evaluated from the FACS data was shown. All data are expressed as the mean ± SD from 3 independent experiments. *$P < .05$ vs GFP-transduced cells by using the Student *t* test.

$p27^{kip1}$ shRNA effectively abolished the inhibitory effect of ADA-FoxO1 on HSC proliferation; (5) PDGF produced intracellular ROS, and transduction of MnSOD inhibited PDGF-induced ROS production and proliferation in HSCs; and (6) $FoxO1^{+/-}$ mice are more susceptible to liver fibrosis after bile duct ligation than wild-type littermates. The transcriptional regulation of transdifferentiation, proliferation, and collagen synthesis in HSCs has been intensely investigated, and several transcription factors were identified that control these processes, such as PPAR-γ, Smad, and Kruppel-like factors.[35] Here, we have identified that Forkhead transcription factor FoxO1 is a key transcription factor that regulates proliferation and transdifferentiation of HSCs and liver fibrosis in vivo.

PDGF is the most potent mitogen for transdifferentiated HSCs during liver fibrosis. The PI3K/AKT pathway is activated by PDGF and is an important intracellular mediator of growth signals in HSCs.[3–5] $p70^{S6K}$ Is a downstream target of the PI3K/AKT pathway in HSC proliferation and collagen gene expression.[5] However, the role of mammalian target of rapamycin (mTOR) still needs to be elucidated. The present study indicates that transcriptionally active (ie, nuclear localized) FoxO1 inhibits PDGF-induced HSC proliferation by the G1 cell cycle arrest, whereas transcriptionally inactive FoxO1 stimulated proliferation. Importantly, transcriptionally inactive Δ256-FoxO1 rescued LY294002-induced growth inhibition. Collectively, FoxO1 is a crucial downstream target of the PI3K/AKT pathway to regulate HSC proliferation.

We showed that insulin also phosphorylated FoxO1 via the IRS-2/PI3K/AKT pathway and stimulated HSC proliferation. Nonalcoholic fatty liver disease (NAFLD) is one of the most common causes of chronic liver injury and fibrosis.[36] Insulin resistance and subsequent hyperinsulinemia are highly associated with NAFLD and are an important risk factor for the progression of fibrosis in NAFLD[37] and chronic hepatitis C.[38] The present study suggests that hyperinsulinemia per se may stimulate HSC proliferation via the PI3K/AKT/FoxO1 pathway and contribute to the progression of fibrosis in patients with NAFLD. Because FoxO1 also determines insulin sensitivity in the liver,[26] possible roles of FoxO1 in both fibrosis and insulin resistance may provide a new insight into the pathophysiology and the treatment of NAFLD.

The mechanism underlying HSC transdifferentiation is quite complex. A recent elegant study demonstrated the

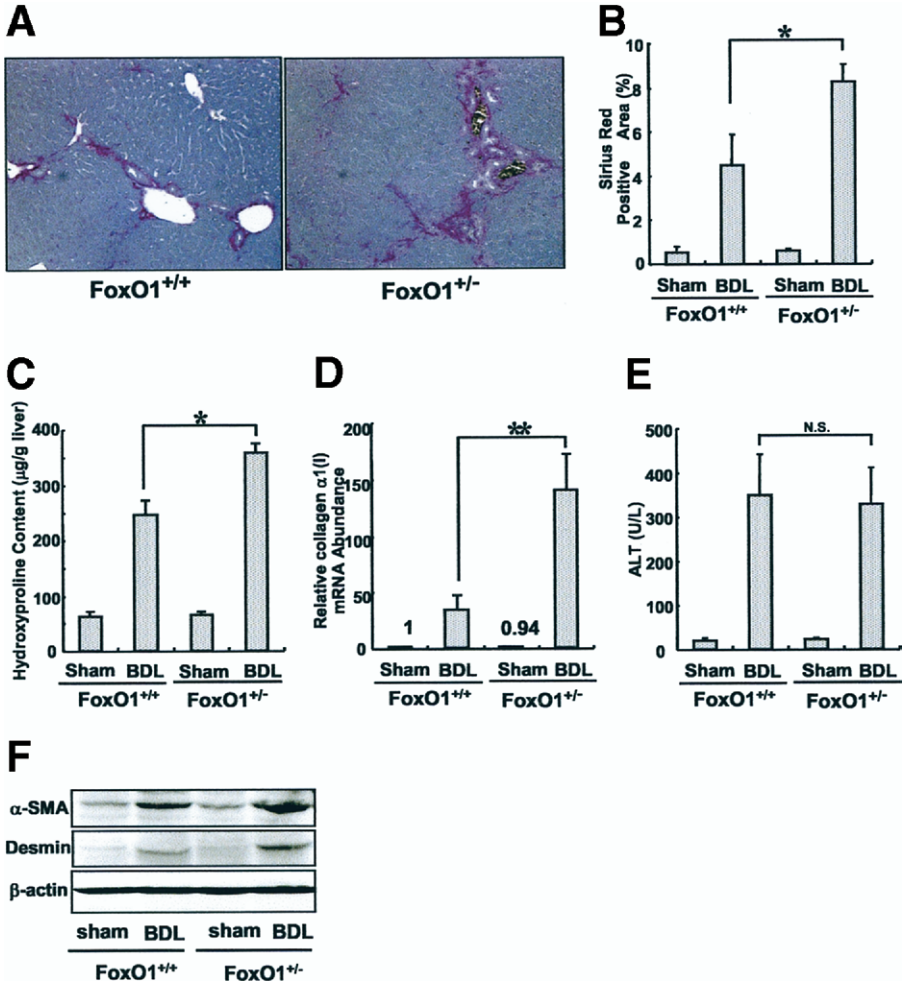

Figure 8. FoxO1 haploinsufficiency enhanced liver fibrosis after BDL. (*A*) Liver sections of FoxO1$^{+/-}$ mice or FoxO1$^{+/+}$ mice 21 days after BDL were stained with Sirius red (original magnification, 40×). The results shown are representative of at least 5 independent experiments. The quantification of percentage Sirius red-positive areas are shown in (*B*), hydroxyproline content on day 21 (*C*), mRNA levels of collagen α1(I) on day 21 (n = 5) (*D*), and serum ALT levels on day 5 (*E*) in sham-operated (sham) and bile duct-ligated (BDL) livers. Five mice were used in each group in each time point. Data are expressed as the mean ± SD. *$P < .05$, **$P < .01$ vs FoxO1$^{+/+}$ mice by using the Student *t* test. (*F*) Western blot analysis for α-SMA and desmin. The results shown are representative of at least 5 independent experiments.

importance of PPAR-γ in maintaining the quiescent HSC phenotype.[32] This study was based on the notion that PPAR-γ is a key transcription factor for adipocyte differentiation[39] and is expressed in the "fat-storing" quiescent HSCs. The expression and activity decreases during HSC transdifferentiation.[11] Because FoxO1 also regulates cellular differentiation including adipocyte differentiation,[13–15] we postulated that FoxO1 contributes to the HSC transdifferentiation process. Indeed, our data demonstrated that ADA-FoxO1 inhibited and Δ256-FoxO1 accelerated the transdifferentiation process of quiescent HSCs. The phosphorylated FoxO1 was increased during their transdifferentiation in culture. Although the mechanism by which phosphorylation of FoxO1 is increased during HSC transdifferentiation is unclear, it is possible that posttranslational modification such as acetylation[25] changes FoxO1 activity during transdifferentiation. Collagen α1(I) expression was also inhibited by ADA-FoxO1 in transdifferentiating HSCs, whereas it was enhanced by Δ256-FoxO1. This inhibitory effect on collagen α1(I) expression may be due to the overall inhibitory effect of FoxO1 on HSC transdifferentiation rather than a direct regulation on collagen α1(I) gene transcription because it was not changed by FoxO1 mutants in transdifferentiated rat HSCs or hTERT HSCs (data not shown).

Among several downstream targets of FoxO1, we identified p27^{kip1} and MnSOD as downstream targets of FoxO1 in HSCs. PDGF or insulin inhibits DNA binding of FoxO1 onto p27^{kip1} and MnSOD promoter regions, resulting in transcriptional inactivation. In contrast, the DNA binding of phosphorylation-resistant ADA-FoxO1 is not inhibited by PDGF or insulin. These findings clearly indicate that transcription of p27^{kip1} and MnSOD is regulated by the PI3K/AKT/FoxO1 pathway in HSCs. In addition to HSC proliferation, p27^{kip1} and MnSOD may also modulate HSC differentiation. As a result of

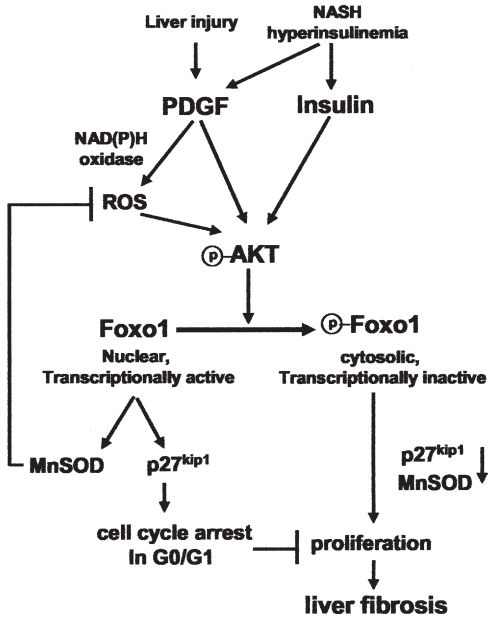

Figure 9. Model of FoxO1 regulation in hepatic stellate cells. During liver fibrosis, PDGF leads to phosphorylation (p) of AKT. Activated AKT phosphorylates FoxO1 leading to their exclusion from the nucleus and preventing FoxO1-dependent gene expression of $p27^{kip1}$ and MnSOD. Downregulation of $p27^{kip1}$ leads HSCs into the S/G2/M phase of cell cycle and proliferation. MnSOD protects excess production of ROS, which are intracellular mediators of proliferation. Hyperinsulinemia in NAFLD patients per se stimulate HSC proliferation via the AKT/FoxO1 pathway.

increased phosphorylation of FoxO1, mRNA levels of $p27^{kip1}$ and MnSOD are decreased during HSC transdifferentiation. The decrease is reversed by ADA-FoxO1 and enhanced by Δ256-FoxO1 (data not shown). $p27^{kip1}$ is an important regulator of cell cycle progression in the G1 phase, supporting our results that FoxO1 inhibits proliferation by G1 cell cycle arrest. In addition, factors that regulate cell cycle can function as a regulator of cellular differentiation.[40,41] Our data demonstrated that shRNA for $p27^{kip1}$ abolished suppressive effect of constitutively active FoxO1 on HSC proliferation. ROS are also an important mediator in proliferation, which can be inhibited by MnSOD.[42] ROS play an important role in hepatic fibrosis.[23,43] Indeed, adenoviral transduction of MnSOD inhibited PDGF-induced ROS production and DNA synthesis. Our results support a previous report that NAD(P)H oxidase-derived ROS plays a crucial role in PDGF-induced proliferation of HSCs.[44] In contrast, insulin did not produce intracellular ROS in HSCs, and transduction of MnSOD did not attenuate insulin-induced HSC proliferation. These data suggest that there are different intracellular signals between PDGF- and insulin-induced growth stimuli in HSCs. Collectively, our data support the notion that $p27^{kip1}$ and, in part, MnSOD are the crucial downstream targets of the PI3K/AKT/FoxO1 pathway to control HSC proliferation and differentiation (Figure 9).

Consistent with the results in culture, we demonstrated that FoxO1 haploinsufficiency increases liver fibrosis in vivo. Although bile duct-ligated $FoxO1^{+/-}$ mice showed no differences in liver injury compared with bile duct-ligated wild-type littermates, $FoxO1^{+/-}$ mice had increased liver fibrosis in vivo. Further studies using other models, such as HSC-specific FoxO1-knockout mice, are required to elucidate more precisely the pathophysiologic significance of FoxO1 functions in liver fibrosis. In conclusion, the present study indicates that the PI3K/AKT/FoxO1 pathway plays a key role in liver fibrosis and thus provides a new direct link between hyperinsulinemia and liver fibrosis. Our work may contribute to the development of novel therapeutic strategies for liver fibrosis induced by the hyperinsulinemia associated with NAFLD.

Appendix

Supplementary Data

Supplementary data associated with this article can be found, in the online version, at doi:10.1053/j.gastro.2007.01.033.

References

1. Bataller R, Brenner DA. Liver fibrosis. J Clin Invest 2005;115:209–218.
2. Scheid MP, Woodgett JR. PKB/AKT: functional insights from genetic models. Nat Rev Mol Cell Biol 2001;2:760–768.
3. Marra F, Gentilini A, Pinzani M, Choudhury GG, Parola M, Herbst H, Dianzani MU, Laffi G, Abboud HE, Gentilini P. Phosphatidylinositol 3-kinase is required for platelet-derived growth factor's actions on hepatic stellate cells. Gastroenterology 1997;112:1297–1306.
4. Reif S, Lang A, Lindquist JN, Yata Y, Gabele E, Scanga A, Brenner DA, Rippe RA. The role of focal adhesion kinase-phosphatidylinositol 3-kinase-akt signaling in hepatic stellate cell proliferation and type I collagen expression. J Biol Chem 2003;278:8083–8090.
5. Gabele E, Reif S, Tsukada S, Bataller R, Yata Y, Morris T, Schrum LW, Brenner DA, Rippe RA. The role of p70S6K in hepatic stellate cell collagen gene expression and cell proliferation. J Biol Chem 2005;280:13374–13382.
6. Accili D, Arden KC. FoxOs at the crossroads of cellular metabolism, differentiation, and transformation. Cell 2004;117:421–426.
7. Brunet A, Bonni A, Zigmond MJ, Lin MZ, Juo P, Hu LS, Anderson MJ, Arden KC, Blenis J, Greenberg ME. Akt promotes cell survival by phosphorylating and inhibiting a Forkhead transcription factor. Cell 1999;96:857–868.
8. Nakamura N, Ramaswamy S, Vazquez F, Signoretti S, Loda M, Sellers WR. Forkhead transcription factors are critical effectors of cell death and cell cycle arrest downstream of PTEN. Mol Cell Biol 2000;20:8969–8982.
9. Medema RH, Kops GJ, Bos JL, Burgering BM. AFX-like Forkhead transcription factors mediate cell-cycle regulation by Ras and PKB through p27kip1. Nature 2000;404:782–787.
10. Vincent KJ, Jones E, Arthur MJ, Smart DE, Trim J, Wright MC, Mann DA. Regulation of E-box DNA binding during in vivo and in vitro activation of rat and human hepatic stellate cells. Gut 2001;49:713–719.
11. Miyahara T, Schrum L, Rippe R, Xiong S, Yee HF Jr, Motomura K, Anania FA, Willson TM, Tsukamoto H. Peroxisome proliferator-activated receptors and hepatic stellate cell activation. J Biol Chem 2000;275:35715–35722.

12. Marra F, Efsen E, Romanelli RG, Caligiuri A, Pastacaldi S, Batignani G, Bonacchi A, Caporale R, Laffi G, Pinzani M, Gentilini P. Ligands of peroxisome proliferator-activated receptor γ modulate profibrogenic and proinflammatory actions in hepatic stellate cells. Gastroenterology 2000;119:466–478.
13. Kitamura T, Nakae J, Kitamura Y, Kido Y, Biggs WH III, Wright CV, White MF, Arden KC, Accili D. The forkhead transcription factor Foxo1 links insulin signaling to Pdx1 regulation of pancreatic β cell growth. J Clin Invest 2002;110:1839–1847.
14. Nakae J, Kitamura T, Kitamura Y, Biggs WH III, Arden KC, Accili D. The forkhead transcription factor Foxo1 regulates adipocyte differentiation. Dev Cell 2003;4:119–129.
15. Hribal ML, Nakae J, Kitamura T, Shutter JR, Accili D. Regulation of insulin-like growth factor-dependent myoblast differentiation by Foxo forkhead transcription factors. J Cell Biol 2003;162:535–541.
16. Siegmund SV, Uchinami H, Osawa Y, Brenner DA, Schwabe RF. Anandamide induces necrosis in primary hepatic stellate cells. Hepatology 2005;41:1085–1095.
17. Schnabl B, Purbeck CA, Choi YH, Hagedorn CH, Brenner D. Replicative senescence of activated human hepatic stellate cells is accompanied by a pronounced inflammatory but less fibrogenic phenotype. Hepatology 2003;37:653–664.
18. Osawa Y, Hannun YA, Proia RL, Brenner DA. Roles of AKT and sphingosine kinase in the antiapoptotic effects of bile duct ligation in mouse liver. Hepatology 2005;42:1320–1328.
19. Nakae J, Kitamura T, Silver DL, Accili D. The forkhead transcription factor Foxo1 (Fkhr) confers insulin sensitivity onto glucose-6-phosphatase expression. J Clin Invest 2001;108:1359–1367.
20. Lehmann TG, Wheeler MD, Froh M, Schwabe RF, Bunzendahl H, Samulski RJ, Lemasters JJ, Brenner DA, Thurman RG. Effects of three superoxide dismutase genes delivered with an adenovirus on graft function after transplantation of fatty livers in the rat. Transplantation 2003;76:28–37.
21. Tamamori-Adachi M, Hayashida K, Nobori K, Omizu C, Yamada K, Sakamoto N, Kamura T, Fukuda K, Ogawa S, Nakayama KI, Kitajima S. Down-regulation of p27Kip1 promotes cell proliferation of rat neonatal cardiomyocytes induced by nuclear expression of cyclin D1 and CDK4. Evidence for impaired Skp2-dependent degradation of p27 in terminal differentiation. J Biol Chem 2004;279:50429–50436.
22. Schnabl B, Kweon YO, Frederick JP, Wang XF, Rippe RA, Brenner DA. The role of Smad3 in mediating mouse hepatic stellate cell activation. Hepatology 2001;34:89–100.
23. Bataller R, Schwabe RF, Choi YH, Yang L, Paik YH, Lindquist J, Qian T, Schoonhoven R, Hagedorn CH, Lemasters JJ, Brenner DA. NADPH oxidase signal transduces angiotensin II in hepatic stellate cells and is critical in hepatic fibrosis. J Clin Invest 2003;112:1383–1394.
24. Daitoku H, Yamagata K, Matsuzaki H, Hatta M, Fukamizu A. Regulation of PGC-1 promoter activity by protein kinase B and the forkhead transcription factor FKHR. Diabetes 2003;52:642–649.
25. Daitoku H, Hatta M, Matsuzaki H, Aratani S, Ohshima T, Miyagishi M, Nakajima T, Fukamizu A. Silent information regulator 2 potentiates Foxo1-mediated transcription through its deacetylase activity. Proc Natl Acad Sci U S A 2004;101:10042–10047.
26. Nakae J, Biggs WH III, Kitamura T, Cavenee WK, Wright CV, Arden KC, Accili D. Regulation of insulin action and pancreatic β-cell function by mutated alleles of the gene encoding forkhead transcription factor Foxo1. Nat Genet 2002;32:245–253.
27. Datta SR, Brunet A, Greenberg ME. Cellular survival: a play in three Akts. Genes Dev 1999;13:2905–2927.
28. Kops GJ, Medema RH, Glassford J, Essers MA, Dijkers PF, Coffer PJ, Lam EW, Burgering BM. Control of cell cycle exit and entry by protein kinase B-regulated forkhead transcription factors. Mol Cell Biol 2002;22:2025–2036.
29. Kops GJ, Dansen TB, Polderman PE, Saarloos I, Wirtz KW, Coffer PJ, Huang TT, Bos JL, Medema RH, Burgering BM. Forkhead transcription factor FOXO3a protects quiescent cells from oxidative stress. Nature 2002;419:316–321.
30. Schmidt M, Fernandez de Mattos S, van der Horst A, Klompmaker R, Kops GJ, Lam EW, Burgering BM, Medema RH. Cell cycle inhibition by FoxO forkhead transcription factors involves down-regulation of cyclin D. Mol Cell Biol 2002;22:7842–7852.
31. Dijkers PF, Medema RH, Lammers JW, Koenderman L, Coffer PJ. Expression of the pro-apoptotic Bcl-2 family member Bim is regulated by the forkhead transcription factor FKHR-L1. Curr Biol 2000;10:1201–1204.
32. Hazra S, Xiong S, Wang J, Rippe RA, Krishna V, Chatterjee K, Tsukamoto H. Peroxisome proliferator-activated receptor γ induces a phenotypic switch from activated to quiescent hepatic stellate cells. J Biol Chem 2004;279:11392–11401.
33. Iredale JP, Benyon RC, Arthur MJ, Ferris WF, Alcolado R, Winwood PJ, Clark N, Murphy G. Tissue inhibitor of metalloproteinase-1 messenger RNA expression is enhanced relative to interstitial collagenase messenger RNA in experimental liver injury and fibrosis. Hepatology 1996;24:176–184.
34. Hosaka T, Biggs WH III, Tieu D, Boyer AD, Varki NM, Cavenee WK, Arden KC. Disruption of forkhead transcription factor (FOXO) family members in mice reveals their functional diversification. Proc Natl Acad Sci U S A 2004;101:2975–2980.
35. Eng FJ, Friedman SL. Transcriptional regulation in hepatic stellate cells. Semin Liver Dis 2001;21:385–395.
36. Angulo P. Nonalcoholic fatty liver disease. N Engl J Med 2002;346:1221–1231.
37. Bugianesi E, Manzini P, D'Antico S, Vanni E, Longo F, Leone N, Massarenti P, Piga A, Marchesini G, Rizzetto M. Relative contribution of iron burden, HFE mutations, and insulin resistance to fibrosis in nonalcoholic fatty liver. Hepatology 2004;39:179–187.
38. Ortiz V, Berenguer M, Rayon JM, Carrasco D, Berenguer J. Contribution of obesity to hepatitis C-related fibrosis progression. Am J Gastroenterol 2002;97:2408–2414.
39. Spiegelman BM, Flier JS. Adipogenesis and obesity: rounding out the big picture. Cell 1996;87:377–389.
40. Drissi H, Hushka D, Aslam F, Nguyen Q, Buffone E, Koff A, van Wijnen A, Lian JB, Stein JL, Stein GS. The cell cycle regulator p27kip1 contributes to growth and differentiation of osteoblasts. Cancer Res 1999;59:3705–3711.
41. Lipinski MM, Jacks T. The retinoblastoma gene family in differentiation and development. Oncogene 1999;18:7873–7882.
42. Sarsour EH, Agarwal M, Pandita TK, Oberley LW, Goswami PC. Manganese superoxide dismutase protects the proliferative capacity of confluent normal human fibroblasts. J Biol Chem 2005;280:18033–18041.
43. Zhong Z, Froh M, Wheeler MD, Smutney O, Lehmann TG, Thurman RG. Viral gene delivery of superoxide dismutase attenuates experimental cholestasis-induced liver fibrosis in the rat. Gene Ther 2002;9:183–191.
44. Adachi T, Togashi H, Suzuki A, Kasai S, Ito J, Sugahara K, Kawata S. NAD(P)H oxidase plays a crucial role in PDGF-induced proliferation of hepatic stellate cells. Hepatology 2005;41:1272–1281.

Received March 20, 2006. Accepted January 4, 2007.

Address requests for reprints to: David A. Brenner, MD, University of California, San Diego Health Sciences, 1318 Biomedical Science Building, 9500 Gilman Drive #0602, La Jolla, California 92093. E-mail: dbrenner@ucsd.edu; fax: (858) 822-0084.

M.A. is the recipient of a Postdoctoral Fellowship of the Uehara Memorial Foundation.

Supported in part by National Institutes of Health (NIH) grants PPG DK59340, R01 AA15055, and R01 GM041804.

The authors thank Drs Akiyoshi Fukamizu and Hiroaki Daitoku (Tsukuba University, Japan) for technical assistance for ChIP assays.